Japanese Journal of Applied Physics
Vol. 44, No. 1A, 2005, pp. 145–146

Brief Communication

Characterization of Low-Temperature Stress Hump in Relation to Phase Formation Sequence of Nickel Silicide

Jeong Eui HONG*, Jeong Soo BYUN[1], Sun Il KIM and Byung Tae AHN

Department of Materials Science and Engineering, Korea Advanced Institute of Science and Technology, 373-1Guseong-dong, Yuseong-gu, Daejon 305-701, Korea
[1]*Applied Materials Inc., 3050 Bowers Avenue, P.O. Box 58039, Santa Clara, CA 95054-3299, USA*

(Received August 26, 2004; accepted September 27, 2004; published January 11, 2005)

The stress hump phenomenon observed at a low temperature of approximately 140°C during *in situ* stress-temperature measurement of sputtered Ni thin film on a (001) Si substrate has been investigated. We found that the stress hump was not related to the formation of $NiSi_2$, but originated from the thickening of an amorphous Ni–Si intermixing layer in the temperature range of 100–140°C followed by the formation of the Ni_2Si phase at temperatures above 140°C.
[DOI: 10.1143/JJAP.44.145]

KEYWORDS: NiSi, stress hump, phase formation sequence, interdiffusion

Nickel monosilicide is the most suitable material for the self-aligned silicide process as device geometry is scaled down to the nano regime due to its well-known advantages.[1,2] Recently, Lauwers *et al.*[1)] and Tsai *et al.*[3)] have reported that the Ni/Si system displayed a stress hump at a low temperature, i.e., below 200°C, which is a unique phenomenon of nickel silicide. Lauwers *et al.* assumed that this could be related to the formation of epitaxial $NiSi_2$ as the first phase during the annealing of Ni thin film (<100 nm) on an implanted (001) Si substrate. A few other authors have also reported the same results.[4–6)] In this study, we analyzed the microstructures of Ni thin film on a (001) Si substrate with various thermal histories in order to characterize the stress hump in relation to the phase formation sequence.

P-type (001) Si wafers with a resistivity of 5–12 Ωcm were used as substrates. A 15 nm-thick Ni film was sputter-deposited on the Si wafers, and followed by Ti or TiN capping of Ni for some of the wafers. Then the wafers were loaded into a vacuum furnace ($<3 \times 10^{-6}$ Torr) equipped with a laser beam on top of the chamber. The total force per unit width (F/W) acting on the metal film was *in situ*-measured during annealing up to 500°C at a ramp-up rate of 6°C/min. To examine the microstructural changes associated with the low-temperature stress hump, samples were prepared with various thermal histories as described in Table I. X-ray diffraction (XRD) analysis, cross-sectional transmission electron microscopy (TEM), and auger electron spectroscopy (AES) were used for analysis. TEM specimens were made by the focused ion beam (FIB) method to maintain the temperature lower than 100°C.

Table I. Annealing conditions for microstructural analysis.

Sample	Annealing conditions
a	As-deposited
b	Annealed up to 120°C, then immediately cooled down
c	Annealed up to 140°C, then immediately cooled down
d	Annealed up to 140°C, then held the temperature for 40 min before being cooled down

*E-mail address: jeong_eui_hong@amat.com

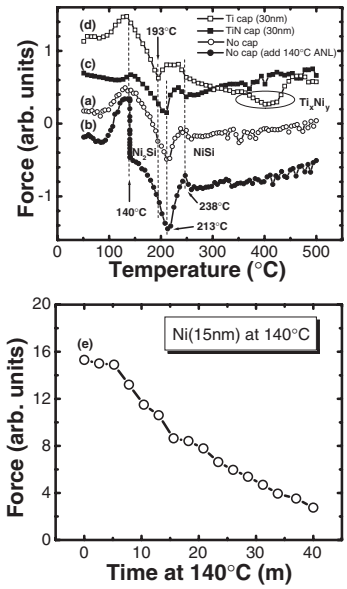

Fig. 1. Total force per unit width (F/W) of Ni 15 nm/Si; (a) No capping, (b) isothermal annealing step added to uncapped sample, (c) TiN cap, (d) Ti cap, and (e) stress relaxation with time during the isothermal annealing at 140°C.

Figure 1 shows the F/W acting on the metal film with increasing temperature. For the uncapped wafers in Fig. 1(a), several inflection points are observed at approximately 100°C, 140°C, 210°C, and 240°C, corresponding to the formation of Ni_2Si, the phase transformation from Ni_2Si to NiSi, and the completion of the phase transformation to NiSi, respectively.[3)] The tensile stress built up in the temperature range of 100–140°C was relaxed almost completely during isothermal annealing at 140°C [Fig. 1(b)] and the stress relaxation with time was close to linearity [Fig. 1(e)]. For the TiN-capped wafer, only a negligible stress hump is observed at low temperature and the overall variation in F/W is also significantly reduced compared with that of the uncapped wafers due to the rigidity of the TiN film. For the Ti-capped wafer, it is shown that the phase transformation from Ni_2Si to NiSi commences at a lower temperature and F/W decreases continuously from 240°C to 400°C, which is presumably related to the formation of the intermetallic compound Ti_xNi_y.

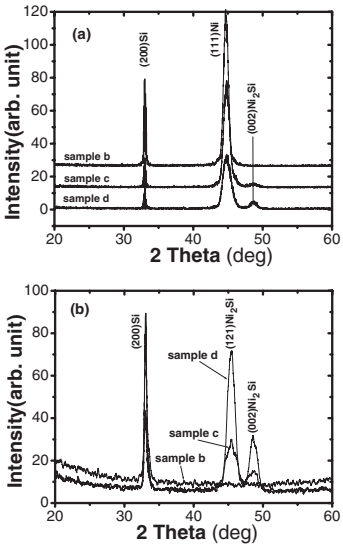

Fig. 2. XRD spectra of Ni 15 nm/Si samples before (a) and after Ni strip-off (b).

In Fig. 2, we present the XRD spectra of the samples as functions of annealing conditions. It is shown that the silicide reaction begins at 140°C and the first phase is Ni_2Si. Comparing sample c and sample d, a sharper and stronger Ni_2Si peak intensity with a decreased Ni peak was observed for sample d, which implies that more Ni reacted with Si to form Ni_2Si with increased crystallinity during isothermal annealing at 140°C. The presence of the Ni_2Si phase and the difference in the peak intensity of Ni_2Si between samples c and d can be seen more clearly when Ni is stripped off selectively [Fig. 2(b)]. The formation of Ni_2Si in this stage is responsible for the decrease in F/W with time at temperatures above 140°C. After annealing up to 500°C, only the NiSi phase was present, regardless of the thermal histories (not shown).

Cross-sectional TEM images are presented in Fig. 3. A thin interlayer is observed between Ni and Si in samples a and b, which is an amorphous Ni–Si mixture with approximately 50% of each element.[7,8] The thicknesses of the amorphous Ni–Si mixture in samples a and b were 3.7 nm and 4.2 nm, respectively. On the other hand, samples c and d consist of bilayers of Ni on top and a mixture of Ni_2Si and amorphous Ni–Si at the interface. While the Ni_2Si and

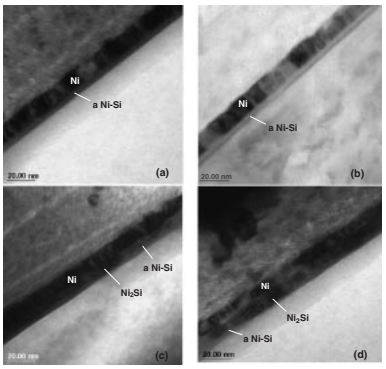

Fig. 3. Cross-sectional TEM images of Ni 15 nm/Si samples; (a) sample a, (b) sample b, (c) sample c, and (d) sample d.

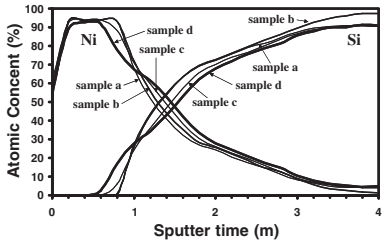

Fig. 4. AES depth profiles of Ni and Si atoms in Ni 15 nm/Si samples as functions of annealing conditions.

amorphous Ni–Si layer in sample c is relatively thin and has amorphous-like contrast, it becomes thicker with more crystalline contrast in sample d [Figs. 3(c) and 3(d)]. Note that there is no faceted interface, which is a typical microstructure of epitaxial $NiSi_2$ on (001) Si observed in all the samples. It should also be noted that there is no interfacial oxide layer between metals and Si.

Figure 4 shows the AES depth profiles of Ni and Si atoms. For sample b, the Ni and Si profiles are almost the same as those of the as-deposited sample except for the slope, which means that Ni and Si atoms interdiffused, resulting in a thicker amorphous Ni–Si mixture without any silicide reaction during annealing up to 120°C. On the contrary, samples c and d have inflection points in the Ni and Si profiles at the point where the atomic concentration ratio of Ni to Si is approximately 2 : 1, corresponding to the formation of Ni_2Si. The difference in the Ni and Si profiles between samples c and d is that Ni_2Si is thicker in sample d than in sample c, which is consistent with the observations from XRD and TEM analyses.

In conclusion, we found that the low-temperature stress hump phenomenon observed during *in situ* stress-temperature measurement of a sputtered Ni thin film on a (001) Si substrate was not related to the formation of $NiSi_2$, but resulted from the thickening of an amorphous Ni–Si intermixing layer caused by interdiffusion of the Ni and Si atoms in the temperature range of 100–140°C. The tensile stress was thereafter relaxed due to the formation of Ni_2Si as the first phase at temperatures above 140°C. Ni_2Si was transformed to NiSi after annealing up to 500°C regardless of the thermal histories.

Acknowledgments

The Korea Science and Engineering Foundation (KOSEF) financially supported this work.

1) A. Lauwers, A. Steegen, M. de Potter, R. Lindsay, A. Satta, H. Bender and K. Maex: J. Vac. Sci. & Technol. B **19** (2001) 2026.
2) A. Lawers, P. Besser, T. Gutt, A. Satta, M. de Potter, R. Lindsay, N. Roelandts, F. Loosen, S. Jin, H. Bender, M. Stucchi, C. Vrancken, B. Deweerdt and K. Maex: Microelectron. Eng. **50** (2000) 103.
3) C. J. Tsai and K. H. Yu: Thin Solid Films **350** (1999) 91.
4) L. J. Chen, C. M. Doland, I. W. Wu, J. J. Chu and S. W. Lu: J. Appl. Phys. **62** (1987) 2789.
5) H. Von Kanel: Mater. Sci. Eng. **8** (1992) 196.
6) V. Teodorescu, L. Nistor, H. Bender, A. Steegen, A. Lauwers, K. Maex and J. Can Landuyt: J. Appl. Phys. **90** (2001) 167.
7) G. B. Kim, D.-J. Yoo, H. K. Baik, J.-M. Myoung, S. M. Lee, S. H. Oh and C. G. Park: J. Vac. Sci. & Technol. B **21** (2003) 319.
8) L. A. Clevenger and C. V. Thompson: J. Appl. Phys. **67** (1990) 1325.